TABLE 2 The Organic Phosphorus Concentration of Dimethoate Solution Change with the Degradation Time

Degradation Time (min)	10	20	30	40	50	60
Organic phosphorus concentration (mg/L)	37.13	30.05	23.85	20.33	15.91	15.87

and so forth, it will take long time to get samples and take the concentration test.

The LPG system has the obvious advantages, for example, real-time monitoring which can improve the efficiency of sewage treatment process can also be implemented due to LPG's fast response and high precision. The LPG is of great significance to the design of new sewage treatment system. The LPG system has some disadvantage too. The demodulation device used in the detection system is the optical spectrum analyzer which is expensive, bulky, and is inconvenient to be carried. In future research, demodulation device which has low cost and small size should be developed for engineering applications.

4. CONCLUSION

Dimethoate solution which belongs to the phosphorodithioate class is chosen as the representative of degradation of organophosphorus pesticides in wastewater. The long-period fiber grating resonant wavelength has a certain good relationship with the concentration of dimethoate solution. Based on it, an on-line real-time monitoring the degradation of dimethoate solution is realized by the LPG. The degradation of dimethoate solution is achieved by the EC technology and ultrasound. The method using long-period fiber grating to measure liquid concentration or refractive index measurement has a simple structure, it can monitor and operate instantaneously. The entire system achieves all-fiber technology, it has a good prospect. The experimental results presented in this article were shown that making use of the LPG is an attractive method of permitting on-line measurements. The research in this article can promote the combination of the fiber-grating sensor technology and the organophosphorus pesticide sewage monitoring technology. In future, we will make some research by coating the LPG with a layer of polymer or metal film to improve on the sensitivity for our target analytes.

ACKNOWLEDGMENT

This work was supported by the key national natural science foundation (Nos. 61201109; 51007002; 51275239) and Anhui Province Key Project of Natural Science Foundation (Nos. KJ2010A341; KJ2011Z031).

REFERENCES

1. D. Pant, Waste glass as absorbent for thin layer chromatography (TLC), Waste Manag 29 (2009), 2040–2041.
2. M. Clariana, M. Gratacós-Cubarsí, M. Hortós, J.A. García-Regueiro, and M. Castellari, Analysis of seven purines and pyrimidines in pork meat products by ultra high performance liquid chromatography–Tandem mass spectrometry, J Chromatogr A 1217 (2010), 4294–4299.
3. I. Kristiana, A. Heitz, C. Joll, and A. Sathasivan, Analysis of polysulfides in drinking water distribution systems using headspace solid-phase microextraction and gas chromatography–mass spectrometry, J Chromatogr A 1217 (P2010), 5995–6001.
4. C. Silva, J.M.P. Coelho, P. Caldas, O. Frazão, P.A.S. Jorge, and J.L. Santos, Optical fiber sensing system based on long-period gratings for remote refractive index measurement in aqueous environments, Fiber Integrated Opt 29 (2010), 160–169.
5. T. Erdogan, Fiber grating spectra, J Lightwave Technol 15 (1997), 1277–1294.
6. V. Bhatia, Applications of long-period gratings to single and multiparameter sensing, Opt Express 4 (1999), 457–466.
7. T. Erdogan, Cladding-mode resonances in short- and long-period fiber grating filters, J Opt Soc Am A 14 (1997), 1760–1773.
8. X. Shu, L. Zhang, and I. Bennion, Sensitivity characteristics of long-period fiber gratings, J Lightwave Technol 20 (2002), 255–266.
9. M.Y.A. Mollah, R. Schennach, J.R. Parga, and D.L. Cocke, Electrocoagulation (EC)—Science and applications, J Hazard Mater B 84 (2001), 29–41.

A MINIATURIZED DUAL-BAND ANTENNA FOR LONG-TERM EVOLUTION SYSTEM TEMPLATE

Chih Peng Lin, T. Y. Lin, Jie-Huang Huang, and Christina F. Jou
School of Communication Engineering Department, National Chiao Tung University, Taiwan; Corresponding author: jadanz.cm96g@gmail.com

Received 26 September 2012

ABSTRACT: *Long-term evolution (LTE) (fourth generation mobile networks) has utilized multiple-input–multiple output (MIMO) technology to achieve very high data rates in both uplink and downlink. MIMO is based on the multiple antenna systems within the small size mobile terminal. One of the challenges is to miniaturize the mobile terminal. In this article, a compact antenna with the dual-band characteristics, which meet the specification of the LTE frequency band (680–900 MHz and 2.28–2.82 GHz) is proposed. The bandwidths of both the lower and the higher frequency bands are 320 and 540 MHz, respectively. The total size of the antenna is 54 × 26.6 mm^2. A fairly good agreement has been shown between the simulation and experimental results. The study on the effect of the various antenna parameters has also been discussed.* © 2013 Wiley Periodicals, Inc. Microwave Opt Technol Lett 55:1379–1382, 2013; View this article online at wileyonlinelibrary.com. DOI 10.1002/mop.27566

Key words: *LTE; MIMO; multiband*

1. INTRODUCTION

In recent years, long-term evolution (LTE) [1, 2] has become a popular mobile network technology after GSM (the second generation mobile networks) and Universal Mobile Telecommunications System (UMTS; the third generation mobile networks). LTE is a project of the third Generation Partnership Project and a set of enhancements to the UMTS. LTE is internet protocol based technology with broader bandwidth, high transmission rate, and less wireless network delay. It will have theoretical peak data rates for downlink of at least 100 Mbps, an uplink of at least 50 Mbps and supporting scalable carrier bandwidths, from 1.4 to 20 MHz.

Generally, there are two operating modes of the LTE system. One is based on time division duplexing (TDD), and the other is based on frequency division duplexing (FDD). FDD using the paired spectrum is anticipated to form the migration path for the current 3G services. TDD using unpaired spectrum is providing the evolution or upgrade path for TD-SCDMA.

For the LTE antenna, designing the lower frequency band will pose some design challenges in the mobile terminal due to size limitations. In this article, the design of the proposed antenna in the lower frequency band is being taken into consideration first, and then the additional technique such as stub and slot are

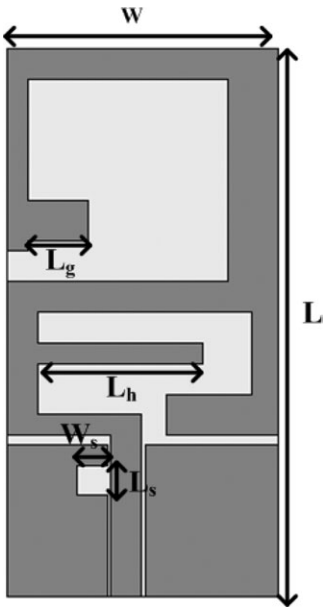

Figure 1 Geometry of the proposed antenna with associated parameters

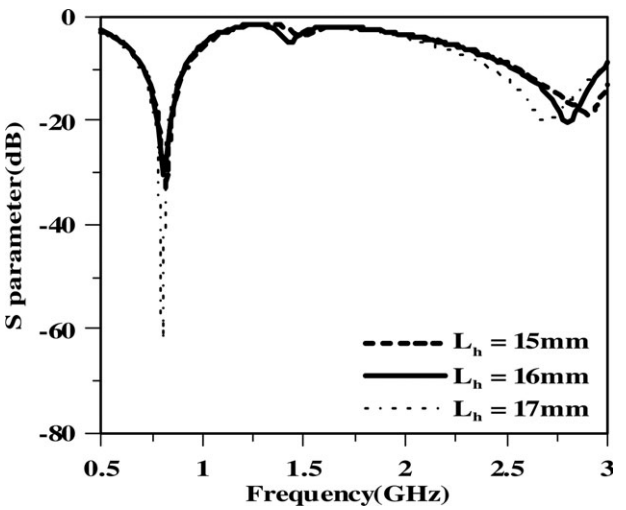

Figure 2 The reflection coefficient variation with different L_h

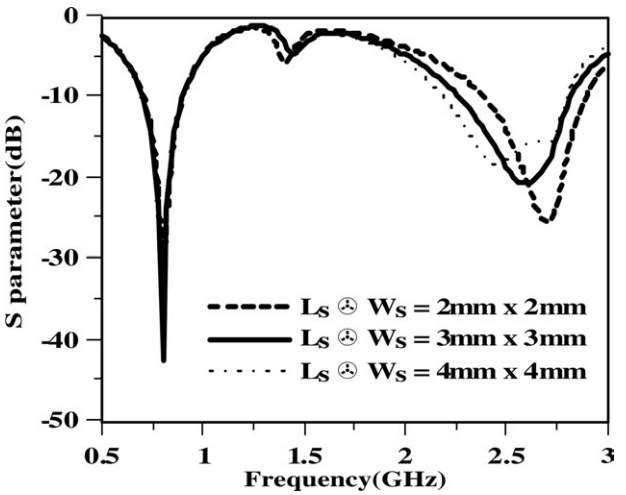

Figure 3 The reflection coefficient variation with different L_s and W_s

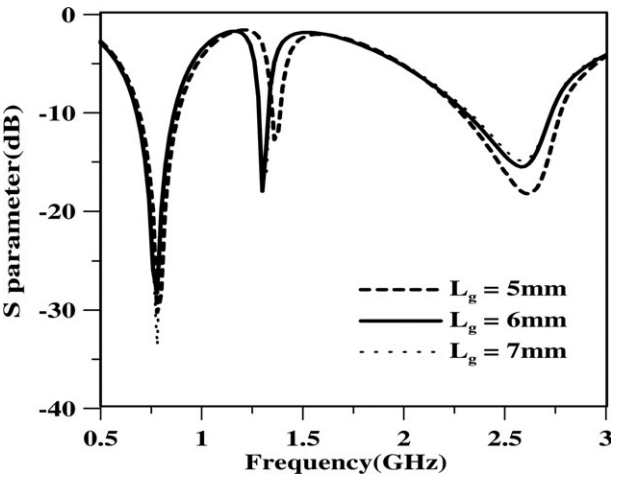

Figure 4 The reflection coefficient variation with different L_g

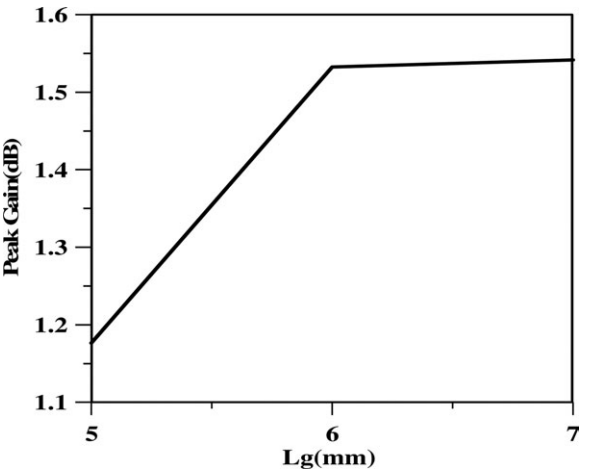

Figure 5 Peak gain value with different L_g

applied to improve the bandwidth and gain in the higher frequency band. The measured results have shown good agreement with the simulated results.

2. ANTENNA DESIGN

The geometry of the proposed antenna is shown in Figure 1. The fed-in is composed of a 50 Ω CPW. The substrate is FR4 with a dielectric constant of 4.4 and the thickness of 0.8 mm.

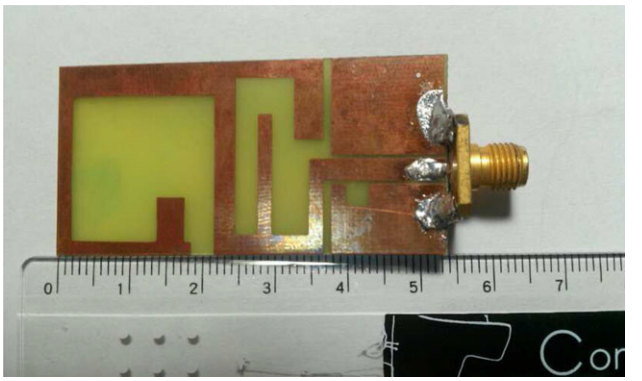

Figure 6 The top view of the fabricated antenna. [Color figure can be viewed in the online issue, which is available at wileyonlinelibrary.com]

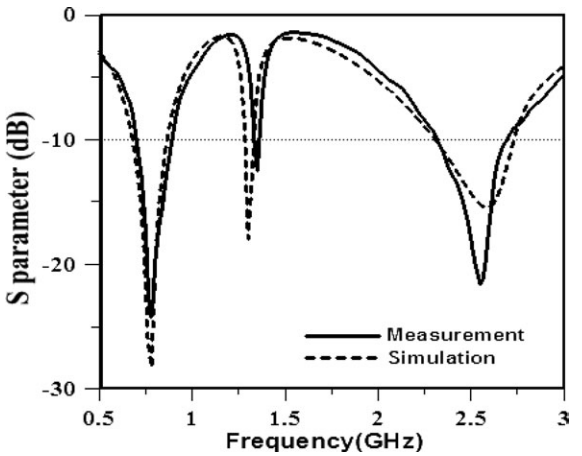

Figure 7 The reflection coefficient of the simulated and the measured result

The first step is to consider the design of the lower frequency band (698–894 MHz). The current distribution of the longest resonant path is about 113.2 mm, which is longer than the quarter wavelength at 800 MHz. The technique has been proposed in Refs. 3 and 4. It can support the operating frequency from 700 to 900 MHz. Second, to achieve the desired LTE frequency band (2.3–2.7 GHz), an additional path L_h is added to create the frequency band at 2.8 GHz. Moreover, a slot is added on the CPW ground plane to increase the bandwidth.

To extend the bandwidth to 2.4 GHz, the stub L_h is added to create the current path from the ground plane to its end about 33 mm, which can resonate around 2.4 GHz. As shown in Figure 2, the simulated S_{11} shifts toward the lower frequency in the higher frequency band as L_h increases. However, the peak gain will decrease as L_h increases. Therefore, the optimized L_h is selected to be 16 mm.

For the slot design [5], varying different sizes of ($L_s \times W_s$) will affect the reflection coefficient as shown in Figure 3. When the size

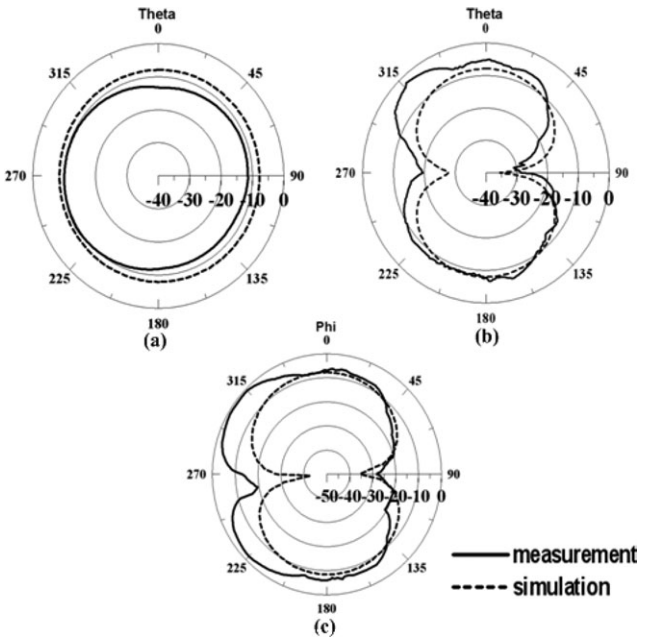

Figure 8 The radiation pattern at 775 MHz in (a) *x*–*z* plane; (b) *y*–*z* plane; and (c) *x*–*y* plane

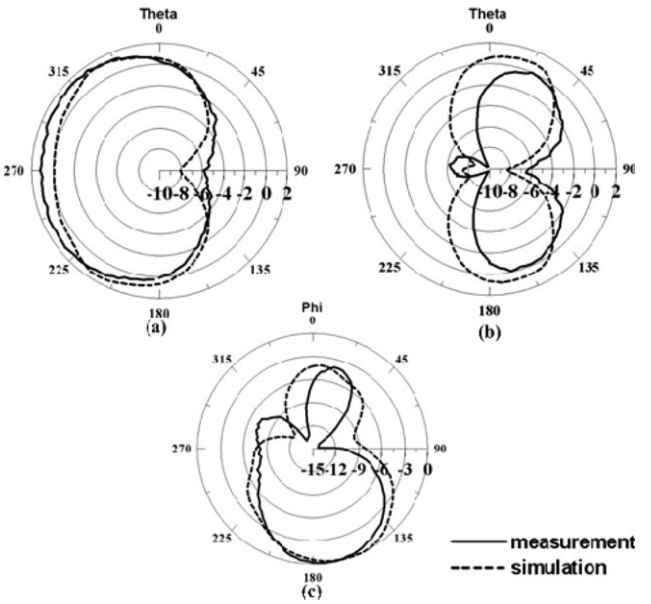

Figure 9 The radiation pattern at 2570 MHz in (a) *x*–*z* plane; (b) *y*–*z* plane; and (c) *x*–*y* plane

of ($L_s \times W_s$) increases, the bandwidth also increases, but the gain will decrease. As $L_s = 4$ mm and $W_s = 4$ mm, the proposed antenna will reach a compromise between the bandwidth and the gain for the higher frequency band (2.3–2.69 GHz) application.

As mentioned earlier, the additional path and the slot on the ground plane are utilized to improve the reflect coefficient in the desire band of the lower frequency band from 680 to 900 MHz and the higher frequency band from 2.28 to 2.82 GHz, respectively. However, the peak gain at the higher frequency band is only 0.3 dB, which is too small for 2.6 GHz application. Therefore, a stub (L_g) is added to increase the gain. The variations on the gain and the S_{11} according to L_g have been shown in Figures 4 and 5, respectively. The peak gain saturates as $L_g = 6$ mm, and meanwhile the S_{11} is only slightly affected.

According to the above discussions, the optimized parametrical values can be decided as follows: $L = 54$ mm, $W = 26.6$ mm, $L_g = 6$ mm, $L_h = 16$ mm, $W_s = 3$ mm, and $L_s = 3$ mm.

3. EXPERIMENTAL VERIFICATION

The fabricated antenna is shown in Figure 6, and the total size of the proposed antenna is 54×26.6 mm^2, which is a fairly compact for the applications below 1 GHz.

The simulated and measured S_{11} is shown in Figure 7. The measured result has shown fairly good agreement with the simulated result. The slight disagreement should be caused by manufacturing errors. The frequency shift in the lower frequency band is only 20 MHz. In the higher frequency band, the bandwidth decreases about 20 MHz, but the S_{11} is improved.

The simulated and the measured radiation patterns at 775 MHz are shown in Figures 8. The conventional monopole pattern and the omnidirectional pattern in the *x*–*z* plane have been shown. The radiation patterns at 2570 MHz are shown in Figure 9. Due to the asymmetric structure of the proposed antenna, the main radiation is in *x* direction.

The simulated peak gain values at 775 and 2570 MHz are −7.7 and 1.5 dB, respectively. The measured gains at each frequency are −10 and 1.2 dB, respectively. Notice that in the LTE system, the minimum acceptable gain is −10 dB, which is the same value as our measured result.

4. CONCLUSION

In this article, a CPW feed, compact size, dual-band antenna for LTE application is presented. The effect on the reflection coefficient according to different design parameters has been shown and discussed. The lower frequency band of the proposed antenna can cover UMTS-800 (830–885 MHz) and GSM850 (824–894 MHz). The higher frequency band can cover IMT-2000 (2300–2400 MHz), bluetooth (2400–2500 MHz), WLAN (2400–2500 MHz), and WiMax (2500–2600 MHz). The total size of the proposed antenna is 54×26.6 mm^2, which is relatively small for the application below 1 GHz.

REFERENCES

1. D. Astely, et al., LTE: The evolution of mobile broadband, IEEE Commun Mag 47 (2009), 44–51.
2. A. Ghosh, et al., LTE-advanced: Next-generation wireless broadband technology, IEEE Wireless Commun 17 (2010), 10–22.
3. W.H. Hsu, et al., Design of a sinuous route monopole antenna for handset, In: IEEE Asia Pacific Microwave Conference, Singapore, 2009, pp. 2791–2793.
4. C.H. Chang and K.L. Wong, Penta-band one-eighth wavelength PIFA for internal mobile phone antenna, In: IEEE Antennas and Propagation Society International Symposium, Charleston, SC, 2009, pp. 1–4.
5. M.A. Antoniades and G.V. Eleftheriades, A compact multiband monopole antenna with a defected ground plane, IEEE Antennas Wireless Propag Lett 7 (2008), 652–655.

MULTIPLE MODE RESONANCE BPF DESIGN USING SUSPENDED STRIPLINE WITH SOURCE-LOAD COUPLING STRUCTURE

Min-Hua Ho,[1] Wanchu Hong,[1] Hong-Yin Lin,[2] and Po-Fan Chen[3]

[1] Graduate Institute of Communications Engineering, National Changhua University of Education, #2, Shih-Da Road, Changhua City, Taiwan 50074, Republic of China; Corresponding author: ho@cc.ncue.edu.tw

[2] Institute of Computer and Communication Engineering, National Cheng Kung University, #1, University Road, Taiwan 70101, Republic of China

[3] King Yuan Electronics Co., Ltd, #81, Section 2, Gongdaowu 5th Road, Hsin-Chu, Taiwan 30070, Republic of China

Received 26 September 2012

ABSTRACT: *A multiple-mode resonance bandpass filter of suspended stripline structure is proposed in this article with a source-load coupling feed design. Equivalent quasilumped elements circuit model is developed to represent the proposed filter's discontinuities and to emulate its frequency responses. The odd- and even-mode equivalent half circuits extracted from the derived LC circuit model are also examined for analyzing the circuit's mode resonances. Multiple resonances, which relate to two odd modes and two even modes, are observed. The circuit's physical layout of the proposed filter is guided by the LC circuits, and then the circuit's dimensions are optimized by sonnet simulation. Experiment is conducted to verify the filter's performance and agreements between the simulations and the measurements are observed.* © 2013 Wiley Periodicals, Inc. Microwave Opt Technol Lett 55:1382–1385, 2013; View this article online at wileyonlinelibrary.com. DOI 10.1002/mop.27565

Key words: *quasilumped element; multiple mode resonance; even/odd mode; suspended stripline; source-load coupling*

1. INTRODUCTION

The suspended stripline (SSL) was first proposed by Rooney and Underkoefler [1] in 1978. It's wide range of realizable characteristic impedances and high-reachable quality factor made itself a very good candidate in building filter of various functions, including low-pass, high-pass, bandstop, and multiplexing. In an SSL configuration, the substrate enclosed by a rectangular metal channel is suspended in air. Hence, most of the SSL's electromagnetic field is distributed in air, benefits the SSL with low loss, high- quality factor, and sharper band edge. In addition, the SSL structure is more flexible in layout because, with the metal housing serves as the ground, the circuit patterns can be deployed on both sides of the substrate. Furthermore, the metal housing provides isolation between the interior circuit and the exterior space, preventing the former from radiating electromagnetic fields into the latter and preventing the electromagnetic noises in the latter from interfering with the former. In building a filter, the housing may be fitted with a variety of RF connectors or be equipped with 50-ohm feed-throughs for direct connection to MICs.

In the past, filters of SSL structure were proposed by Mobbs and Rhodes[2, 3], who built filters and diplexers in various forms. Recently, Menzel and coworkers [4–7] designed SSL filters and diplexers using quasilumped approach. In their quasilumped approach, a few lumped inductive and capacitive elements accounting for the effects of discontinuities in an SSL component and for the electric or magnetic coupling effects between two adjacent SSL components were used to establish an equivalent LC circuit. Those lumped-element circuit models characterized the resonance frequencies of coupled SSL resonators. However, in calculating the entire scope of frequency response, full-wave simulations were unavoidably required in the entire design process.

In fact, full-wave simulations can be engaged in the last stage during the circuit design, whereas the quasilumped approach is extensively used. For given filter specifications, a circuit-layout configuration is proposed first, and subsequently a corresponding meaningful LC circuit model representing the complete filter structure can be established. The element values of the equivalent LC circuit can then be optimized using a circuit-level simulator (e.g., ADS). Once these LC element values are obtained, the structural dimensions of the circuit layout can be adjusted accordingly because there is a meaningful correspondence between each lumped circuit element and some specific part of the circuit layout. It is only in this stage that a full-wave simulator is required.

In this article, an multiple-mode resonance (MMR) bandpass filter (BPF) of SSL structure is presented to achieve a wideband response. To demonstrate the flexibility of the design, a source-load coupling for enhancing signal selectivity of the passband is incorporated in the BPF design. For that purpose, the SSL resonator is printed on the side opposite to the feed lines extended from the signal lines of the SMA connectors, thus allowing the two feed lines to be brought closer to establish the source-load coupling without increasing the circuit size. For the proposed BPF, a circuit layout is proposed first and is followed by the establishment of the corresponding quasilumped circuit. Experiments are conducted to verify the BPF design and agreements are observed between the measured and simulated data.

2. MULTIPLE MODE RESONANCE BPF DESIGN

The proposed BPF is shown in Figure 1 with the circuit configuration originated from Ref. 8, which attaches two narrow strips